Number 3 Volume 16 September 2010 Journal of Engineering

THREE-DIMENSIONAL FINITE ELEMENT ANALYSES OF A SINGLE PILE IN AN ELASTOPLASTIC CLAYEY SOIL

Omar al-Farouk Salem al-Damluji,
Department of Civil Enginering,
University of Baghdad.

Usama Saeed Al-Anbaki,
Former Postgraduate Student,
Department of Civil Engineering,
University of Baghdad.

ABSTRACT

A three-dimensional coupled finite element analysis algorithm is developed to predict the behaviour of single piles in clay. Three dimensional 20-noded brick elements are used in the analyses carried out on three documented field studies. Each node carries four degrees of freedom, three being for displacements in the three perpendicular space dimensions while the fourth is allocated for pore water pressure. The behaviour of the material of the pile is idealized through a linear elastic constitutive relationship while that for the soil by the Modified Cam-Clay model both extended to cover three-dimensional characteristics. The load-displacement results from the developed algorithm on the three selected problems from literature show a very good agreement with the observations. Moreover, the build-up of pore fluid pressures and their dissipations were found to be consistent with field measurements also.

الخلاصة

لقد تم تطوير حسابات تحليل باستخدام طريقة العناصر المحددة المزدوجة بالاتجاهات الثلاثة لتوقع تصرف الركائز المنفردة في الترب الطينية. لقد تم استخدام عناصر طابوقية ذات 20 عقدة بالابعاد الثلاثة لتحليل ثلاثة دراسات حقلية موثقة. تحمل كل عقدة في العنصر المحدد اربعة درجات للحرية, ثلاثة منها للازاحات بالابعاد الثلاثة المتعامدة و الرابعة لضغط ماء المسام. يتم تمثيل التصرف التكويني لمادة الركيزة باستخدام العلاقة الخطية في حين للتربة الطينية بنظرية طين كام المعدلة بعدما تم توسيعها لتشتمل على التصرف بالابعاد الثلاثة. تظهر نتائج الثقل-الازاحة من الحسابات المطورة توافقاً جيداً مع المشاهدات الحقلية. كما تم التوصل على ان النتائج المستحصلة من التحليل لضغط ماء المسام متوافقة مع القياسات الحقلية ايضاً.

KEYWORDS: coupled analysis, finite element, Cam-clay, three dimensional brick elements, load-settlement, pore-water pressure

- PREVIOUS WORKS

As an introduction, a review of literature is made for the behaviour of a single pile in clayey soils and under static loading.

- <u>Analysis of Piles by the Finite Element Method</u>:- Randolph and Wroth *(1978)* used the finite element method to model the manner in which a pile transfers load to the soil for analysis of deformation of vertically loaded piles. Good agreement was obtained between the results of the analysis and solutions obtained from available numerical methods and noticed that the shear stress around the pile decreases in an inverse proportion to the radius. **Desai** *(1978)* studied the effects and simulation of driving of piles into saturated soil media. A procedure for numerical simulation of driving is proposed. Consolidation caused by changes in stress and in pore water pressures, which are obtained on the basis of the *cavity expansion approach*, in the soil mass due to driving was solved using a finite element procedure. **Kuhlemeyer** *(1979)* presented a formulation for an approximation to bending of beams of circular cross sections by the use of the finite element method. The three-degree of freedom characteristic of the element permits an efficient solution to the three dimensional problem of lateral displacement and rotation of transversely loaded circular beams. The high accuracy of the element was confirmed by studying the deflection of cantilever beams subjected to lateral loads. **Kirby and Esrig** *(1979)* used an elastic finite element analysis for pile loading and suggested that the changes in pore pressure associated with changes in mean normal total stress are small and probably in the order of (5-10%) of the undrained shear strength of the soil. Measured pore pressures due to pile loading are typically (0-25%) of the undrained shear strength. **Cooke et al.** *(1979)* described a series of tests made on instrumented tubular steel piles in the field to examine the mechanism of load transfer from piles in stiff clay. During installation of the first pile, loading tests were made to piles in stiff clay. During installation of the first pile, loading tests were made so that the variation of the soil properties and the effect of pile length on settlements at corresponding working loads could be examined. **Ottaviani and Marchetti** *(1979)* compared results obtained from a loading test on cast-in-place piles with those obtained from a non-linear finite element analysis based on geotechnical parameters of cohesive soils. The comparison found a good agreement for the loads before failure (allowable) but, there are differences in the loads close to failure (ultimate). **Grande and Nordal** *(1979)* used the finite element method to deal with long term pile head loads. Formulae concerning the ultimate and service load components were derived. In addition to these, equations describing deformations and soil reaction coefficients were introduced. **Randolph et al.** *(1979)* made a numerical analysis of an installation of a single pile driven into clay and the effects on the distribution of stresses and displacements in the soil near the piles immediately after driving and during subsequent consolidation of the clay. The installation of driven piles with the expansion of a *cylindrical cavity* was modelled. The path applied to elements of soil in this process, a strain controlled path, consists, for a typical clay deposit of large lateral extent, of one-dimensional consolidation followed by plane strain constant volume shearing with the plane of shearing being perpendicular to the previous direction of consolidation (rapid installation of the pile). The consolidation of the soil was studied using a work-hardening elasto-plastic soil model, namely, *the Cam-clay model*. **Pal and Parikh** *(1980)* used a finite element analysis for an axially loaded pile-clay system in the elastic region with a computer program capable to handle non-homogeneous and homogeneous clays as well as different pile geometries and different pile penetrations. It was seen that as **L/H** (which is the ratio of the pile length to the total depth of the soil) ranges between **0.75** to **1.00**, there would be an increase in the rate of settlement for a specific slenderness ratio of pile. Morever, it was observed that in the case of full penetration, the amount of load transferred at the base shows a tremendous increase.

Bhowmik and Long *(1990)* presented results of *nonlinear finite element analyses* of an axial pile load test using a *bounding surface plasticity model* to simulate the soil behaviour. The interface between the pile and the surrounding soil is modelled by using thin isoparametric elements. The comparison between observed and predicted pile behaviour is presented and the sensitivity of the analytical solutions to the properties of interface elements is investigated and discussed. The soil-interface-pile model used in this analysis provides a good simulation of the load test analyzed. **Phoon et al.** *(1990)* used the finite element method to study the effect of a spatially varying soil medium on the settlement of single-pile foundations. The soil is assumed to be linear-elastic and it is modelled as a homogeneous field. Using a first-order second-moment technique, the mean and coefficient of variation of the pile head settlement were determined. It is found that the uncertainty of the pile head settlement is dependent on both deterministic and stochastic parameters. Analysis is then performed to compute the reliability index and the corresponding probability of unserviceable behaviour. **Yasser and Hassiotis** *(2001)* developed a three-dimensional, nonlinear finite element model. It is used to study stresses on piles and pile-soils. The model consists of soil continuum elements according to a *Mohr-Coloumb failure criterion* with material nonlinearities for the piles and soil, respectively. The objective of that investigation was to study the mechanism of pile-soil interaction. **Al-Marsumi** *(2003)* developed four algorithms to calculate the total stress, pore water pressure in addition to inclusion of earthquake effects. A three dimensional finite element method was used to analyze the pile-soil system. A single pile with cap and a group of piles with cap were studied while the soil was represented as a homogeneous isotropic and non-homogeneous anisotropic material using the *Modified Cam-Clay model*. **Maharaj et al.** *(2004)* analyzed piles of varying cross-sections by a nonlinear finite element method under plane strain conditions. The soil was modelled by an elasto-plastic medium incorporating *Drucker-Prager* yield criterion. It was found that the load carrying capacity of a single pile is more than that of a pile in a group in case of piles under uplift load and of varying cross-section. **Raheem** *(2005)* used the finite element method to study the behaviour of axially loaded piles embedded in a clayey soil and studying the pore water pressure developed with a thin layer interface element using the *Cam-Clay* model. It was concluded that during undrained loading conditions, the vertical settlement values at the tip of the pile increased in the order of 22.5% when slip elements are used. **Al-Baghdadi** *(2006)* developed a three-dimensional, nonlinear finite element computer program to model soil-pile-raft systems with interface elements between the pile and the surrounding soil. A twenty-noded isoparametric brick element was used. The behaviour of the piled raft material is simulated by using a linear elastic model. However, the behaviour of soil and interface materials is simulated by an elasto-plastic model using the *Mohr-Coulomb failure criterion.*

In this paper, a solution to the problem is proposed by using the *Modified Cam-Clay model* for the soil and the *linear elastic model* for the material of the pile both extended to cover three dimensional conditions.

- DIFFERENTIAL EQUATIONS GOVERNING THE PROBLEM:-

Biot, (1941) developed a three-dimensional consolidation theory based on elastic theory. The assumptions of *Terzaghi-Rendulic* theory are adopted here except that the total stress is allowed to vary within the soil mass although the applied load remains constant. *Biot*'s theory includes the compressibility of the fluid and the soil skeleton and it also deals with

partly saturated soils. For saturated soils, *Biot*'s theory for general three-dimensional problems may be expressed as (Biot 1955, 1956):-

- **Equilibrium Equation:-** For static analysis, the equilibrium equation is (Smith and Griffiths, 1988):-

$$K\frac{d\bar{u}}{dt} + L\frac{d\bar{p}}{dt} - C - \frac{df}{dt} = 0 \quad \ldots\ldots (1)$$

When encountering a non-porous material like concrete, the above equation reduces to:

$$\{F\} = [K].\{\delta\} \quad \ldots\ldots (2)$$

where:- {F}= vector of nodal forces,
[K] = stiffness matrix, and
{δ}= vector of nodal displacements.

The element stiffness matrix for Equation (1) is given by (Smith and Griffiths, 1998):-

$$K = \int_{\Omega} [B]^T [D][B] d\Omega \quad \ldots\ldots (3)$$

where:- [D]= the stress-strain (constitutive) matrix,
[B]= the strain-displacement matrix,
dΩ= the domain of the integration, and
the superscript (^{T}) represents the transpose of the matrix.

Equation (3) can be rewritten in a three-dimensional *local form* as follows:-

$$K = \int_{-1}^{+1}\int_{-1}^{+1}\int_{-1}^{+1} [B]^T [D][B].\det J.d\xi\, d\eta\, d\zeta \quad \ldots\ldots (4)$$

- **Fluid Flow Equation:-** This equation is applied onto flow of water in porous materials like soils only. It can be written as (Lewis and Schrefler, 1987):-

$$H\bar{p} + S\frac{d\bar{p}}{dt} + L^T\frac{d\bar{u}}{dt} - \bar{f} = 0 \quad \ldots\ldots (5)$$

- **Governing Element Matrix Equation:-** By augmenting equations (1) and (5), the following matrix equation is obtained (Lewis and Schrefler, 1987):

$$\begin{bmatrix} K & L \\ L^T & S+\alpha H\Delta t_k \end{bmatrix}_{k,\alpha} \begin{Bmatrix} \bar{u} \\ \bar{p} \end{Bmatrix}_{t_k+\Delta t_k} = \begin{bmatrix} K & L \\ L^T & S-(1-\alpha)H\Delta t_k \end{bmatrix}_{k,\alpha} \begin{Bmatrix} \bar{u} \\ \bar{p} \end{Bmatrix}_{t_k} + \begin{Bmatrix} \frac{df}{dt}+C \\ \bar{f} \end{Bmatrix}_{k,\alpha} \Delta t_k \quad \ldots\ldots (6)$$

The above equation represents the equation governing the soil medium surrounding the pile.

THREE-DIMENSIONAL BRICK ELEMENT:-

In this paper, the problems under consideration are discretized into three-dimensional twenty-node brick elements. Each node in this element has three degrees of freedom representing displacements in the **x**, **y**, and **z**-directions, as well as an additional fourth degree of freedom for pore water pressure.

For the derivation of the required matrices and vectors, the coordinates and local displacement fields of an element are interpolated using polynomials as follows (Owen and Hinton 1980):-

For the three displacement components **u**, **v**, and **w**:-

$$\begin{Bmatrix} u \\ v \\ w \end{Bmatrix} = \begin{bmatrix} [\mathrm{N}] & 0 & 0 \\ 0 & [\mathrm{N}] & 0 \\ 0 & 0 & [\mathrm{N}] \end{bmatrix} \begin{Bmatrix} \delta_i \\ \delta_i \\ \delta_i \end{Bmatrix} \quad \text{.....(7)}$$

Also for three coordinates **x**, **y**, and **z**:-

$$\begin{Bmatrix} \mathrm{x} \\ \mathrm{y} \\ \mathrm{z} \end{Bmatrix} = \begin{bmatrix} [\mathrm{N}] & 0 & 0 \\ 0 & [\mathrm{N}] & 0 \\ 0 & 0 & [\mathrm{N}] \end{bmatrix} \begin{Bmatrix} \mathrm{x}_i \\ \mathrm{y}_i \\ \mathrm{z}_i \end{Bmatrix} \quad \text{..... (8)}$$

where:- $\{\mathrm{u}\} = \{\mathrm{u} \quad \mathrm{v} \quad \mathrm{w}\}^{\mathrm{T}}$, vector of global displacements in the **x**, **y**, and **z**-directions, respectively,

m = number of nodes per element,

$\{\delta_i\}$ = nodal global displacements of node (i),

$\{\mathrm{x}\} = \{\mathrm{x} \quad \mathrm{y} \quad \mathrm{z}\}^{\mathrm{T}}$ vector of global coordinates at any point,

$\{X_i\}$ = vector of global coordinates of nodal point (i), and

$\{N_i\}$ = interpolation function of nodal point (i) (as functions of local coordinates **ξ**, **η**, and **ζ**).

For *small strain theory*, the strain vector for a three-dimensional stress analysis can be written as (Reddy, 1984): -

$$\{\varepsilon\} = \begin{Bmatrix} \varepsilon_x \\ \varepsilon_y \\ \varepsilon_z \\ \gamma_{xy} \\ \gamma_{yz} \\ \gamma_{zx} \end{Bmatrix} = \begin{Bmatrix} \frac{\partial \mathrm{u}}{\partial \mathrm{x}} \\ \frac{\partial \mathrm{v}}{\partial \mathrm{y}} \\ \frac{\partial \mathrm{w}}{\partial \mathrm{z}} \\ \frac{\partial \mathrm{u}}{\partial \mathrm{y}} + \frac{\partial \mathrm{v}}{\partial \mathrm{x}} \\ \frac{\partial \mathrm{v}}{\partial \mathrm{z}} + \frac{\partial \mathrm{w}}{\partial \mathrm{y}} \\ \frac{\partial \mathrm{w}}{\partial \mathrm{x}} + \frac{\partial \mathrm{u}}{\partial \mathrm{z}} \end{Bmatrix} \quad \text{..... (9)}$$

The evaluation of the strain vector requires the evaluation of the derivatives given in Equation (7). The derivatives are calculated by using a *Jacobian transformation matrix*, which relates global coordinates **x**, **y** and **z** derivatives to local coordinate **ξ**, **η**, and **ζ** derivatives (Bathe, 1996):-

$$\begin{Bmatrix} \frac{\partial}{\partial \xi} \\ \frac{\partial}{\partial \eta} \\ \frac{\partial}{\partial \zeta} \end{Bmatrix} = [\mathrm{J}]^{\mathrm{e}} \begin{Bmatrix} \frac{\partial}{\partial \mathrm{x}} \\ \frac{\partial}{\partial \mathrm{y}} \\ \frac{\partial}{\partial \mathrm{z}} \end{Bmatrix} \quad \text{..... (10)}$$

where:-

$[\mathrm{J}]^{\mathrm{e}}$= the Jacobian matrix in Cartesian coordinates.

The *strain-displacement relation* is given as:-

$$\{\varepsilon\} = \sum_{\mathrm{i}=1}^{\mathrm{m}} [\mathrm{B}_\mathrm{i}] \{\delta_\mathrm{i}\} \quad \text{..... (11)}$$

where:-

$[B_i]$= The strain-nodal displacement matrix described by:-

$$[B_i]=\begin{bmatrix} N_{1,1} & 0 & 0 & N_{2,1} & ... & 0 \\ 0 & N_{1,2} & 0 & 0 & ... & 0 \\ 0 & 0 & N_{1,3} & 0 & ... & N_{m,3} \\ N_{1,2} & N_{1,1} & 0 & N_{2,2} & ... & N_{m,1} \\ N_{1,3} & 0 & N_{1,1} & N_{2,3} & ... & N_{m,1} \\ 0 & N_{1,3} & N_{1,2} & 0 & ... & N_{m,2} \end{bmatrix} \quad \text{..... (12)}$$

In the above:-

$$N_{i,j}=\frac{\partial N_i}{\partial x_j} \quad \text{(the first derivative of the shape function).}$$

The three normal and the three shearing stresses are related to the corresponding strains through the stress-strain constitutive matrix **[D]**:-

$$\{\sigma\}=[D]\{\varepsilon\} \quad \text{..... (13)}$$

CONSTITUTIVE RELATIONSHIPS:-

- **Elastic Model:-** Elastic behaviour of a material occurs when no residual strains are retained after unloading, and the material returns to its original shape (Atkinson and Bransby, 1978). In the case of a three-dimensional continuum, it may be expressed in terms of two constants **(K)** and **(G)** as follows (Saada, 1974)**:-**

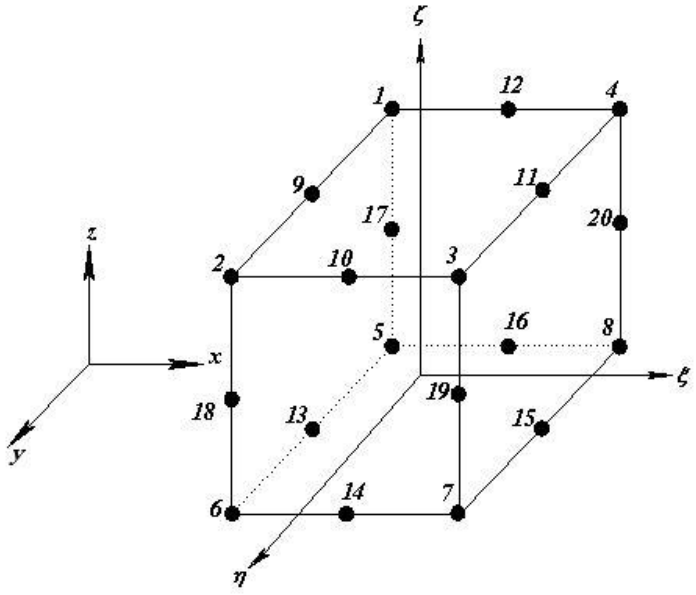

Local Node Number	ξ	η	ζ
1	-1	-1	1
2	-1	1	1
3	1	1	1
4	1	-1	1
5	-1	-1	-1
6	-1	1	-1
7	1	1	-1
8	1	-1	-1
9	-1	0	1
10	0	1	1
11	1	0	1
12	0	-1	1
13	-1	0	-1
14	0	1	-1
15	1	0	-1
16	0	-1	-1

17	-1	-1	0
18	-1	1	0
19	1	1	0
20	1	-1	0

Figure (1) Twenty-node brick element.

$$D=\begin{bmatrix} K+\frac{4}{3}G & K-\frac{2}{3}G & K-\frac{2}{3}G & 0 & 0 & 0 \\ K-\frac{2}{3}G & K+\frac{4}{3}G & K-\frac{2}{3}G & 0 & 0 & 0 \\ K-\frac{2}{3}G & K-\frac{2}{3}G & K+\frac{4}{3}G & 0 & 0 & 0 \\ 0 & 0 & 0 & 2G & 0 & 0 \\ 0 & 0 & 0 & 0 & 2G & 0 \\ 0 & 0 & 0 & 0 & 0 & 2G \end{bmatrix} \quad \text{.....(14)}$$

where:- K= Bulk modulus = $\frac{E}{3(1-2\nu)}$ .....(15)

G= Shear modulus = $\frac{E}{2(1+\nu)}$ .....(16)

In all analyses considered in this paper, the material of the pile, which is concrete, is assumed to follow the constitutive relation described by equation (14).

- **Elasto-Plastic Analysis:-** The relationship between increments of stress and increments of strain for elasto-plastic materials is given by the following equation (Desai and Siriwardane, 1984):-

$$\delta\varepsilon = D^{ep}\delta\sigma' \quad \text{.....(17)}$$

where **δσ'** and **δε** are increments of effective stress and total strain (elastic and plastic), respectively and **(D^{ep})** is the elasto-plastic constitutive matrix. In this study, the critical state model is applied. Since this model requires an *associative flow rule*, where the plastic potential surface is equal to the yield surface (**Q≡F**), the following equation is derived (Al-Damluji, 1981):-

$$d\sigma' = \left[D^e - \frac{D^e \frac{\partial F}{\partial \sigma'} \left\{ \frac{\partial F}{\partial \sigma'} \right\}^T D^e}{\left[-\left\{ \frac{\partial F}{\partial \varepsilon^p} \right\}^T \frac{\partial F}{\partial \sigma'} + \left\{ \frac{\partial F}{\partial \sigma'} \right\}^T D^e \frac{\partial F}{\partial \sigma'} \right]} \right] d\varepsilon \quad \text{.....(18)}$$

- **Modified Cam-Clay Model:-** The *Modified Cam-clay model* addresses the much particular dissatisfaction with the original *Cam-Clay* one. Its yield surface is an ellipse in the meridional plane, shown in Figure (2), and is defined by the equation (Lewis and Schrefler, 1987):-

$$F = \frac{q'^2}{M_{cs}^2} - 2p'p'_c\left(\varepsilon_v^p\right) + p'^2 = 0 \quad \text{.......... (19)}$$

in which $\mathbf{M_{cs}}$ is the slope of the critical state line in the ($\mathbf{p'}$, $\mathbf{q}$) plot, $\mathbf{p'_c}\left(\boldsymbol{\varepsilon_v^p}\right)$ is the preconsolidation pressure to which the soil has previously been subjected to during its past history. It represents the current semi-diameter of the ellipse in the p′-direction.

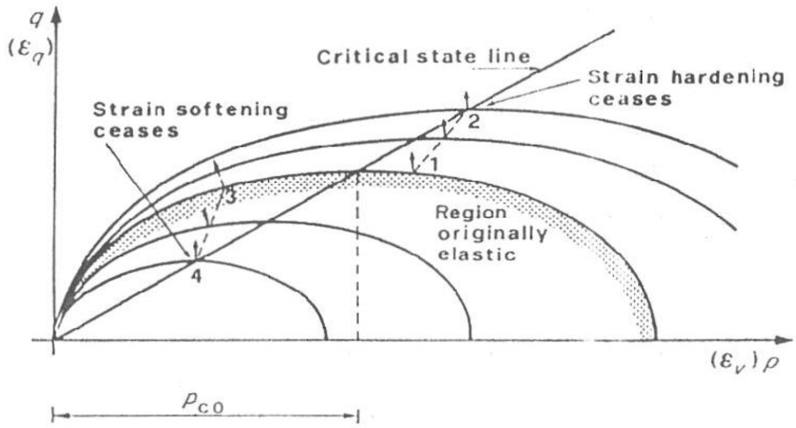

Figure (2) Modified Cam-clay model in the space of two stress invariants q and p.

(after Lewis and Schrefler, 1987)

Clays surrounding piles in the problems solved in this paper are assumed to obey equations (18) and (19). Al-Anbaki (2006) presented all the necessary extensions of the derivations to cover three-dimensional behaviour.

PRESENTATION OF RESULTS:-

After checking the validity of the elastic and elasto-plastic consolidation schemes and the ability of the developed computer program, which was given the name DARC3 (Al-Anbaki, 2006), the present section will discuss the observation results for three field problems documented in literature and compare them with the proposed algorithm output predictions.

-Properties, Geometry and Boundary Conditions:- The pile material used through the following three problems is concrete obeying a linear elastic constitutive relationship as depicted by Equation 14. While for soil, the type of clay involved is modelled by an elasto-plastic *Modified Cam-clay* constitutive relationship as presented by Equation 18. The soil is assumed to be homogeneous and isotropic. The water table is assumed to be at ground level. As the pile section is circular, the meshes used are for a quarter of a cylinder medium. The boundary conditions for the problems are restrained from lateral movement for all nodes while they are free in vertical movements except at the bottom of the mesh. For pore water pressures, they are restrained only at the bottom of the mesh at the circumference.

- **Case Study Number One-Single Pile Analysis (After Desai, 1978):-** This problem is

analyzed according to the research presented by Desai (1978) in which a simulation of driving a pile in a saturated clayey soil is proposed. A discussion of the consolidation process in the soil mass due to changes in stresses and pore water pressures employing dissipations during driving and after subsequent loadings is presented through a nonlinear finite element solution.

- **Mesh and Geometry:-** Figure (3) shows the three-dimensional finite element mesh for a quadrant of a single pile medium with a diameter of (0.4066m) and length of embedment of (15.25m). The depth of the clay layer is (27.452m). It is assumed to extend in the x and y directions about (3.352m) away from the centre of the pile. The total number of three dimensional brick elements employed is (324) and the total number of nodes is (895). Figure (4) shows the x-z plane of the problem while Figure (5) shows the x-y plane.

- **Problem Properties:-** The material properties adopted for this problem are presented in Table (1).

- **Loading:-** The total uniformly distributed load (working load) applied vertically on the top of the pile is (1700) kN/m^2 which is equal to (45%) of the ultimate bearing capacity of the pile of (3800) kN/m^2. The load is applied after (31.1) days from driving of the pile. Through the results presented in this work, the load is assumed to be applied immediately after the installation of the pile.

- **Results:-**

a. Load-Settlement Curve:-

The load-settlement comparison curves at the tip of the pile between the results obtained from the Desai (1978) and these obtained through the current work are shown in Figure (6). It can be seen from the figure that the curves seem to be similar in shape and the difference ratio between the results at the end of loading stage is about (**15%**). Generally, the load-settlement curve seems to be very close to the linear relation behaviour at the

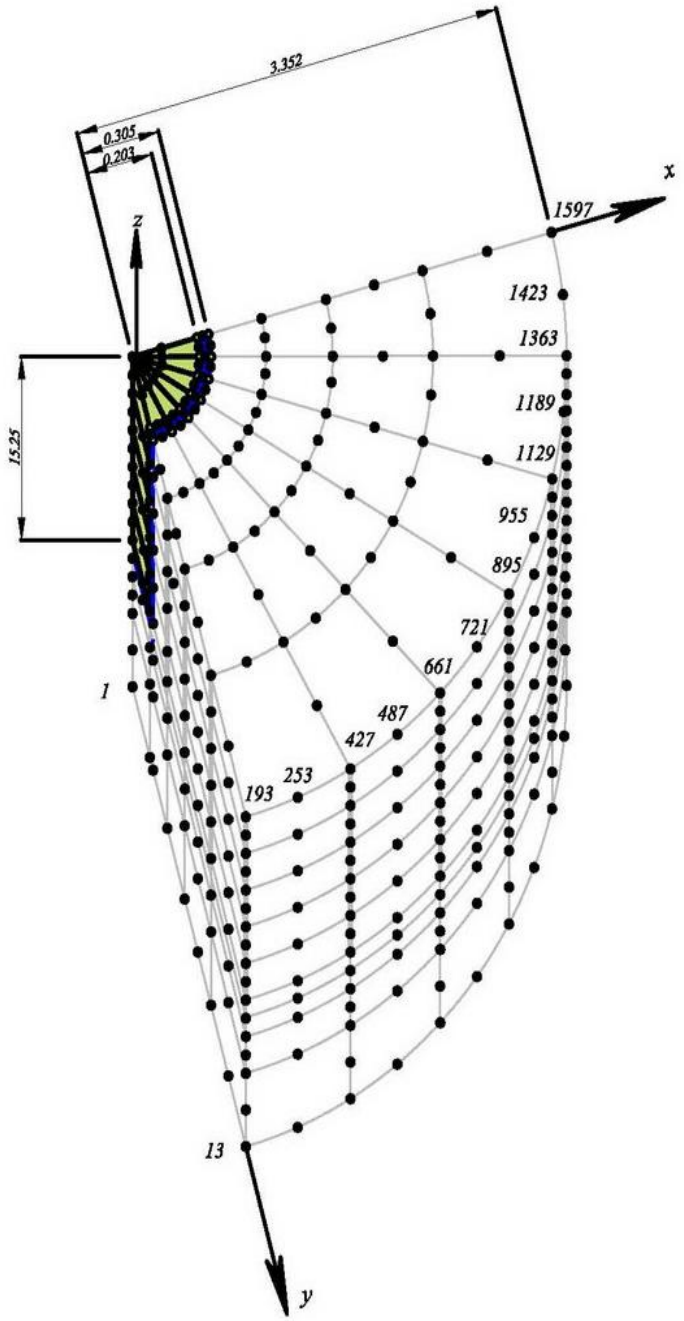

Figure (3) Three- Dimensional finite element mesh for a pile- soil quadrant

initial stage. This may be attributed to the very small pile displacements due to small load increments. As the loading level is increased, the curve tends to show a non-linear relation with smaller slopes (higher settlement values).

b. Pore Water Pressure Dissipation:- Figure (7) shows the pore water pressure dissipation behaviour around the pile at location surface **A-A** shown in Figure (4) for different time steps. The distribution of the excess pore water pressure becomes uniform after considerable time. This may be attributed to the concentration of stresses and strains close to the pile tip. Figure (8) shows the pore water pressure dissipation obtained by Desai (1978). It can be noticed that there is a similarity in the shapes of the pore water pressure curves between these obtained from the current study and the ones concluded by Desai (1978) for time steps greater than (31.1) days. The difference may be attributed to the load which has been applied (31.1) days after installation by Desai (1978) while it is assumed to be applied immediately in the current study.

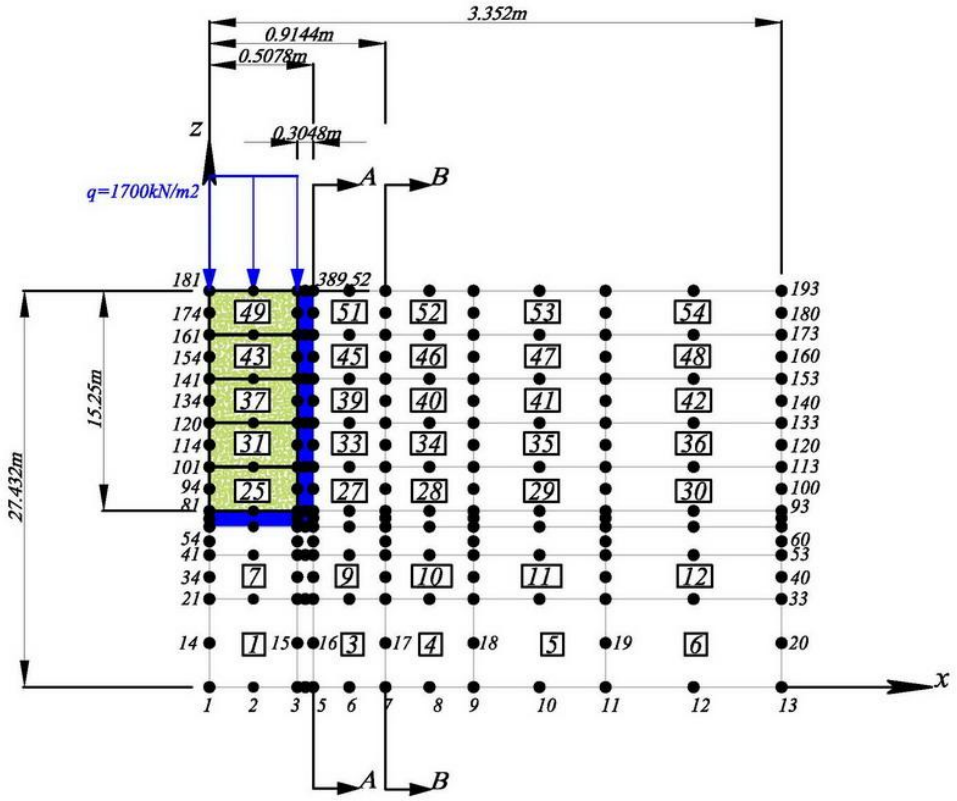

Figure (4) x-z Plane of the Problem

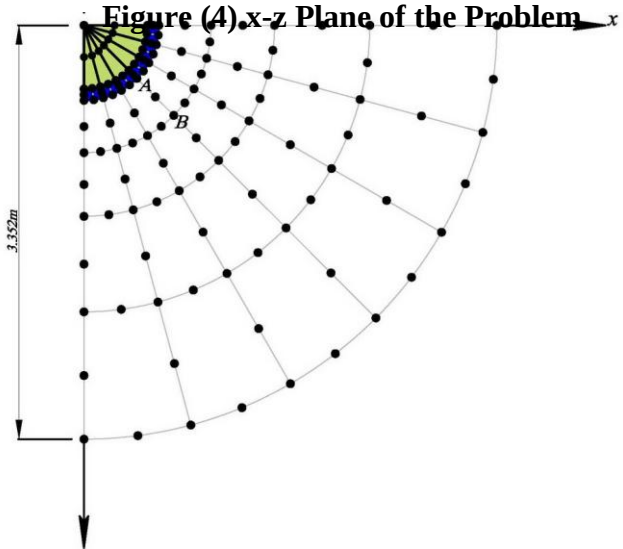

y

Figure (5) x-y plane for problem number one.

Table (1) Material properties for case study number one (from Desai, 1978).

Soil Properties	
Property	**Value**
Undrained strength, $\mathbf{c_u}$	490 lb/ft^2 (23.9 kN/m^2)
Modulus of elasticity of the soil, $\mathbf{E_{soil}}$	44100 lb/ft^2 (2150 kN/m^2)
Poisson's ratio of the soil, $\boldsymbol{\nu_{soil}}$	0.35
The adhesion factor, $\boldsymbol{\alpha}$	1.0
Normal consolidation line slope, $\boldsymbol{\lambda}$	0.17
Shear modulus, **G**	15200 lb/ft^2 (725 kN/m^2)
Pore water pressure parameter in the triaxial state of stress, **A**	1
Unit weight of the soil, $\boldsymbol{\gamma_{soil}}$	110 lb/ft^3 (17.5 kN/m^3)
Permeability coefficient, $\mathbf{k_x=k_y=k_z}$	0.638×10^{-4} ft/day (20×10^{-6} m/day)
Pile Properties	
Property	**Value**
Modulus of elasticity of the pile, $\mathbf{E_{pile}}$	4.32×10^8 lb/ft^2 (21×10^6 kN/m^2)
Poisson's ratio of the pile, $\boldsymbol{\nu_{pile}}$	0.2
Unit weight of the pile, $\boldsymbol{\gamma_{pile}}$	150 lb/ft^3 (24.0 kN/m^3)
Interface Element Properties	
Property	**Value**
Modulus of elasticity of the interface, $\mathbf{E_{interface}}$	44100 lb/ft^2 (2150 kN/m^2)
Poisson's ratio of the interface, $\boldsymbol{\nu_{interface}}$	0.41
Unit weight of the interface, $\boldsymbol{\gamma_{interface}}$	110 lb/ft^3 (17.5 kN/m^3)
Adhesion, $\mathbf{c_a}$	0.3 (kPa)
Wall friction angle, $\boldsymbol{\delta}$	30^o

In Figure (9), the pore water pressure dissipation is calculated at location surface B-B shown in Figure (4). It is evident that values of the pore water pressures in section B-B are not much different from those obtained at section A-A. This may be attributed to the boundary conditions governing the problem and the small distance between the two

sections.

c. <u>Load Distribution Around The Pile</u>:- Figure (10) shows the distribution of the load around the pile and at the tip for different depths and for several values of the load applied at the head of the pile.

- <u>Case Study Number Two-Single Pile Analysis (After Ottaviani and Marchetti, 1977)</u>:- A three-dimensional finite element mesh is used similar to Ottaviani and Marchetti's (1977) two-dimensional discretization. In that paper, results are compared between field data and those obtained from the finite element analysis conducted on the same problem. Analysis by the procedure proposed herein will be presented below.

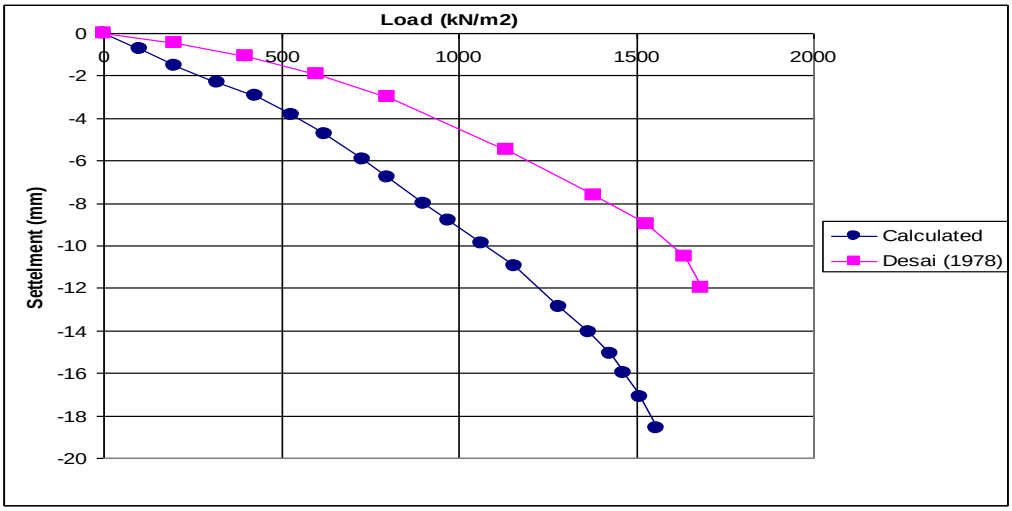

Figure (6) Load-settlement curve.

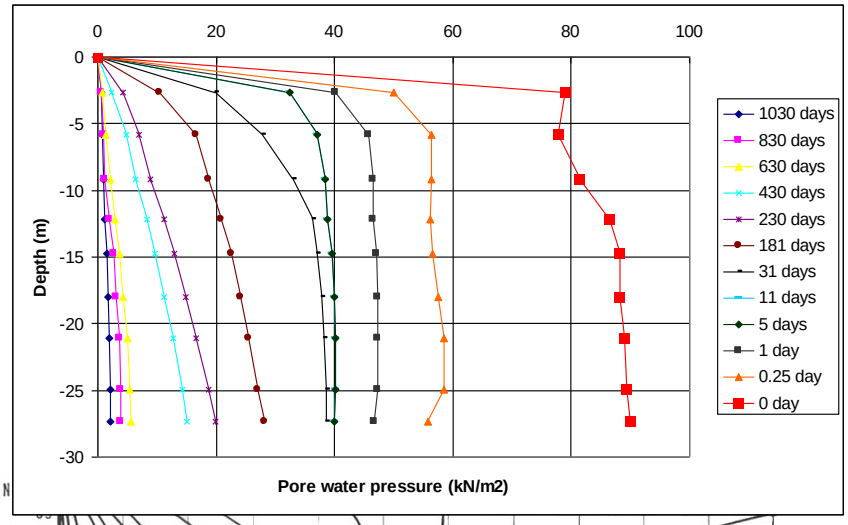

Figure (7) Excess pore water pressure for section A-A.

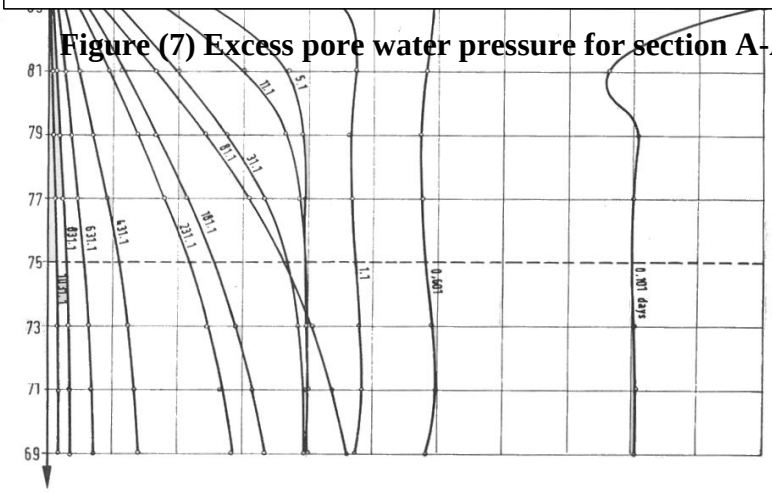

Figure (8) Excess pore water pressures for section A-A (after Desai, 1978), ($1kN/m^2=0.04788LB/FT^2$).

- **Mesh and Geometry**:- Figure (11) shows the three-dimensional finite element mesh for the single pile in clay with a diameter of (0.6)m and length of embedment of (23.5)m. The depth of the clay layer is (32)m. It is assumed to extend in the x and y directions about (4.5)m. The total number of three-dimensional brick elements employed in the current analysis is (1584) and the total number of nodes is (9993).

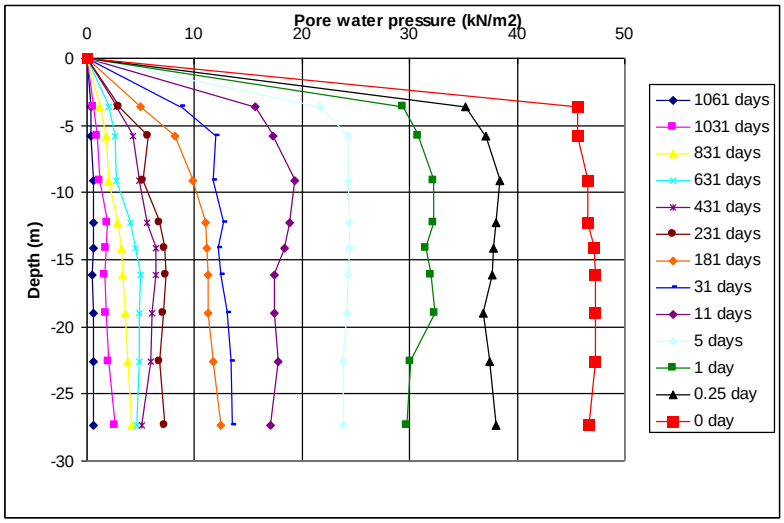

Figure (9) Excess pore water pressure for section B-B.

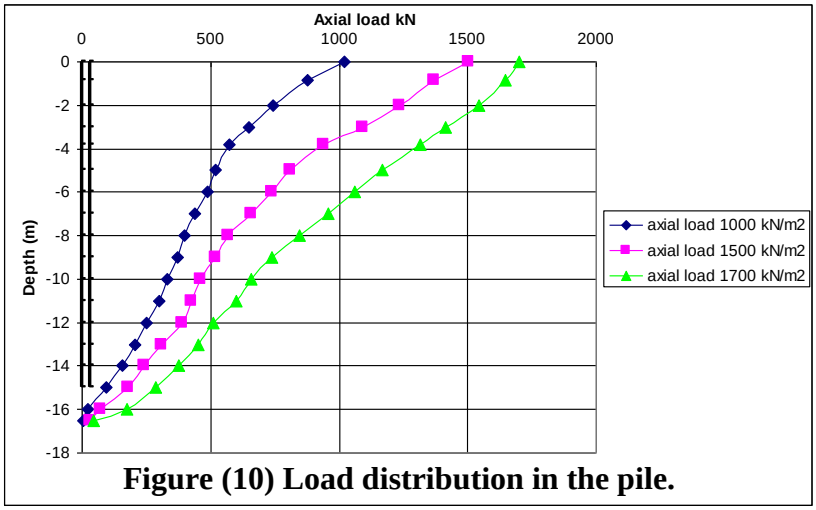

Figure (10) Load distribution in the pile.

- **Soil and Pile Properties**:- The material properties for this problem are presented in Table (2). Figure (12) shows the geotechnical properties of the soil at the location of the pile. It should be noted that during this study, the soil is assumed to be a homogeneous

layer of a clayey deposit and that the properties of the thin layers of sand and the silt are neglected.

- **Loading:-** The total load applied vertically on the top of the pile is (3400) kN which is the ultimate load applied onto the pile.

- **Results:-**

a. Load-Settlement Curve:- Figure (13) shows a comparison between the load-settlement curve for the tip of the pile obtained from the current analysis and that predicted from strain cells at site. It shows a good agreement between the developed algorithm and the measured results. The percentage of differences between the two curves is about (8%) at ultimate load.

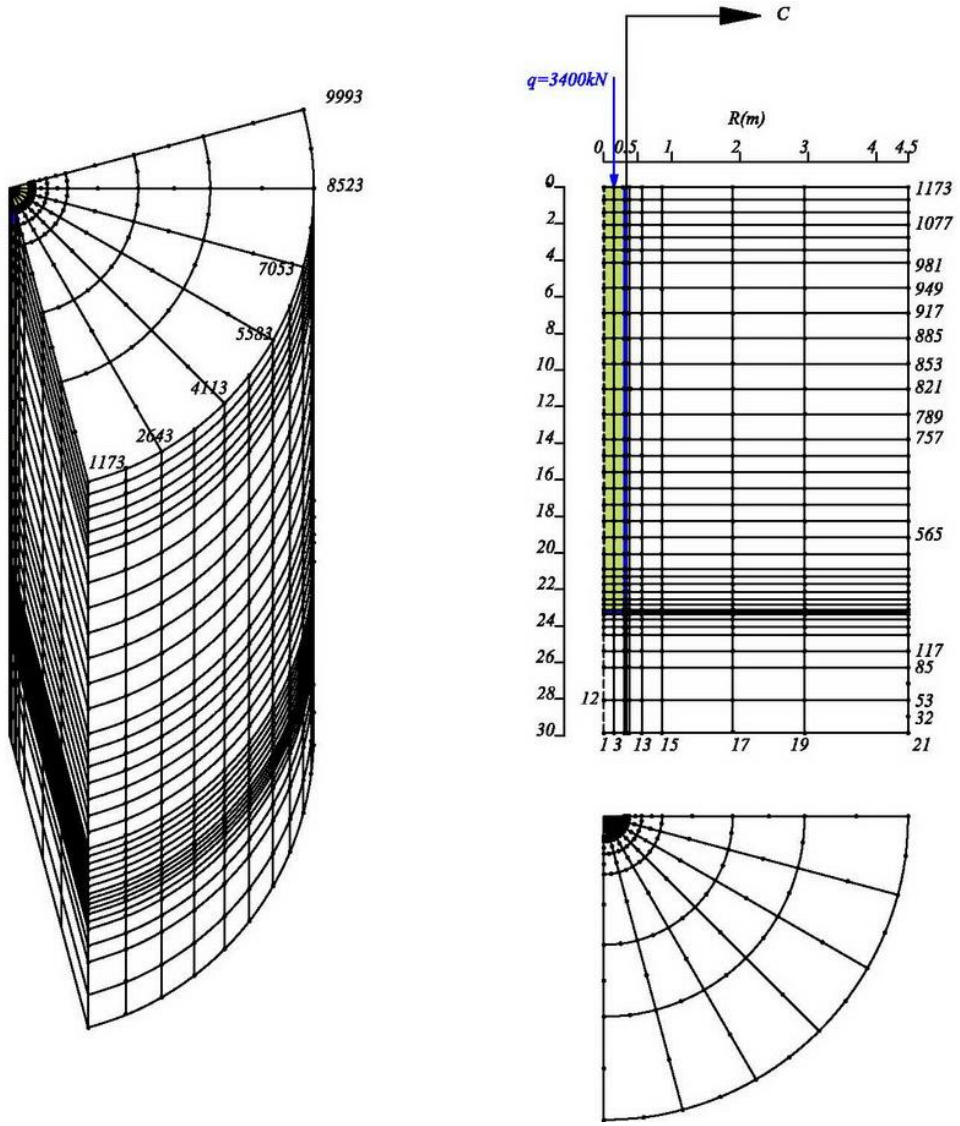

Figure (11) Finite element mesh for the single pile in clay after Ottaviani and Marchetti, 1979.

b. Pore Water Pressure Dissipation:- Figure (14) shows the pore water pressure

dissipation at section C-C near the pile for different time steps. The curves seemed uniform and this may be attributed to the concentration of stresses and strains near the pile.

c. Load Distribution Around the Pile:- Figure (15a-d) shows a comparison of the distribution of the load around the pile between the observed and calculated at different depths for several values applied at the head of the pile. As can be noticed, a good agreement between the observed and the calculated bearing capacities is obtained for small load values while there are some differences under high loads.

Table (2) Material properties for case study number two (after Ottaviani and Marchetti, 1977).

Soil Properties	
Property	**Value**
Undrained strength, c_u	120 kN/m^2
Modulus of elasticity of the soil, E_{soil}	1700 kN/m^2
Poisson's ratio of the soil, ν_{soil}	0.35
The adhesion factor, α	1.0
Normal consolidation line slope, λ	0.15
Unit weight of the soil, γ_{soil}	18.5 kN/m^3
Permeability coefficient, $k_h=k_v$	0.2×10^{-4} m/day
Pile Properties	
Property	**Value**
Modulus of elasticity of the pile, E_{pile}	2.2×10^{7} kN/m^2
Poisson's ratio of the pile, ν_{pile}	0.25
Unit weight of the pile, γ_{pile}	23.5 kN/m^3
Interface Element Properties	
Property	**Value**
Modulus of elasticity of the interface, $E_{interface}$	2000 kN/m^2
Poisson's ratio of the interface, $\nu_{interface}$	0.45
Unit weight of the interface, $\gamma_{interface}$	18.5 kN/m^3
Adhesion, c_a	92 (kPa)
Wall friction angle, δ	32^o

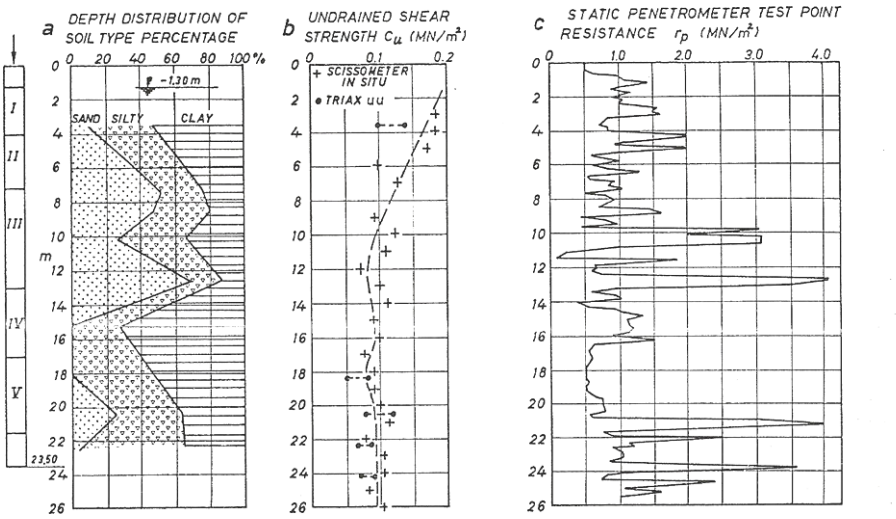

Figure (12) Geotechnical properties of case study number two after Ottaviani and Marchetti, (1979).

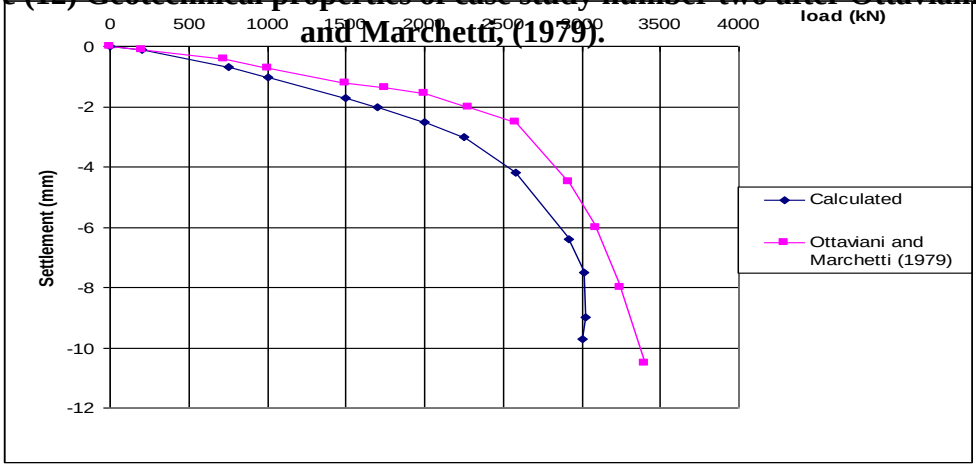

Figure (13) Load-settlement curve.

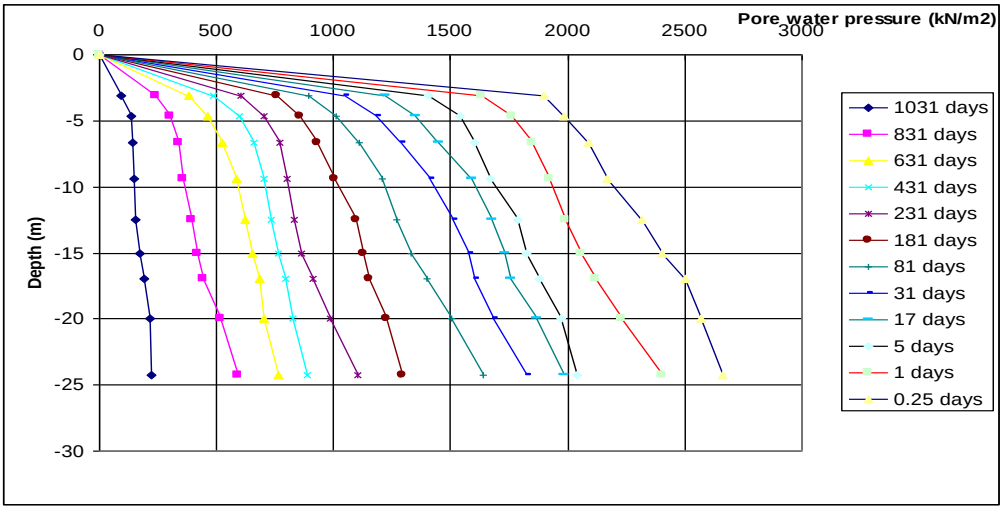

Figure (14) Pore water pressure dissipation.

- Case Study Number Three-Single Pile Analysis (After Seed and Reese, 1955):- This problem is analyzed according to the research conducted by H. Bolton Seed and Lymon C. Reese (1955).

- Mesh and Geometry:- Figure (16) shows the three-dimensional finite element mesh for a single pile in clay with a diameter of (0.1524 m) and length of embedment of (22m).

- Soil and Pile Properties:- The material properties for this problem are presented in Table (3).

- Loading:- The total load applied vertically at the top of the pile is (8000) kN which is the ultimate applied load onto the pile.

- Results:-

a. Load-Settlement Curve:- Figure (17) shows a comparison among the load-settlement curve for the tip of the pile obtained from the present study and those predicted from the strain cells at site in addition to the finite element analysis results presented by the authors. A good agreement shows among these curves. The difference ratio between the curve obtained from the current finite element analysis and the observed values at end of loading is about (25%).

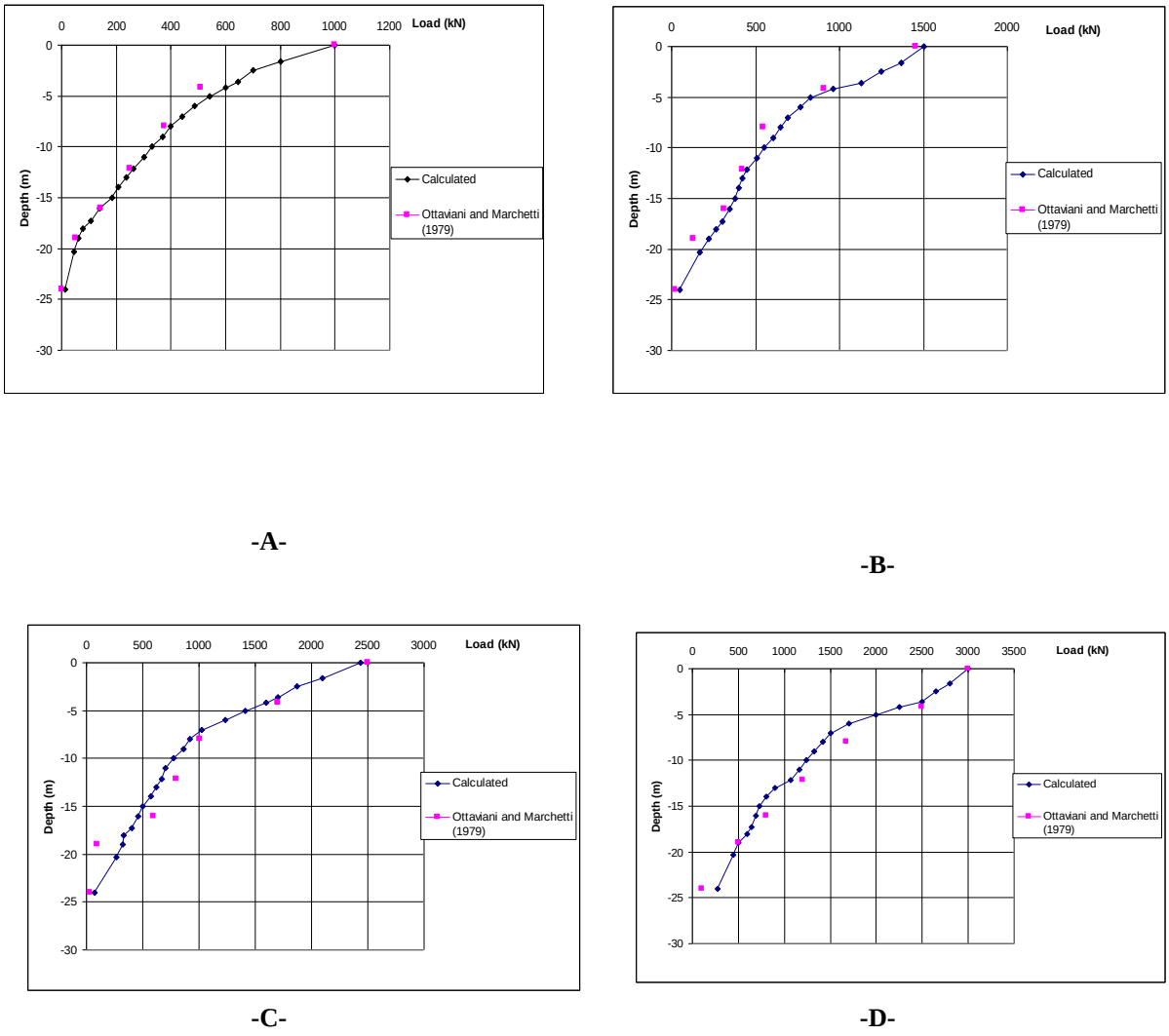

Figure (15) Load distribution in the pile.

b. Pore Water Pressure Dissipation:- Figure (18) shows the pore water pressure

dissipation at section C-C near the pile for different time steps. The study conducted by Seed and Reese did not include pore water pressure measurements.

c. Load Distribution Around The Pile:- Figure (19) shows the distribution of the load in the pile at different depths for several values of the load applied at the head of the pile. The load-distribution curves for the pile showed that most of the load was removed from the pile by shaft resistance while only approximately 10% of the load reached the pile tip. The increased rate of load transfer was exhibited by soil strata at all depths. The load-distribution curves for all loadings showed a general increase in the rate of load transfer with depth with no load being removed by the soil near the ground surface.

CONCLUSIONS:-

The following conclusions can be drawn herein with regard to the results obtained for the analysis of a single pile in elastoplastic clayey soils in three dimensions:

1. For the single pile driven in clay analyzed by Desai (1978), when applying the developed algorithm based on ACED3 program herein, the following results have been obtained:-

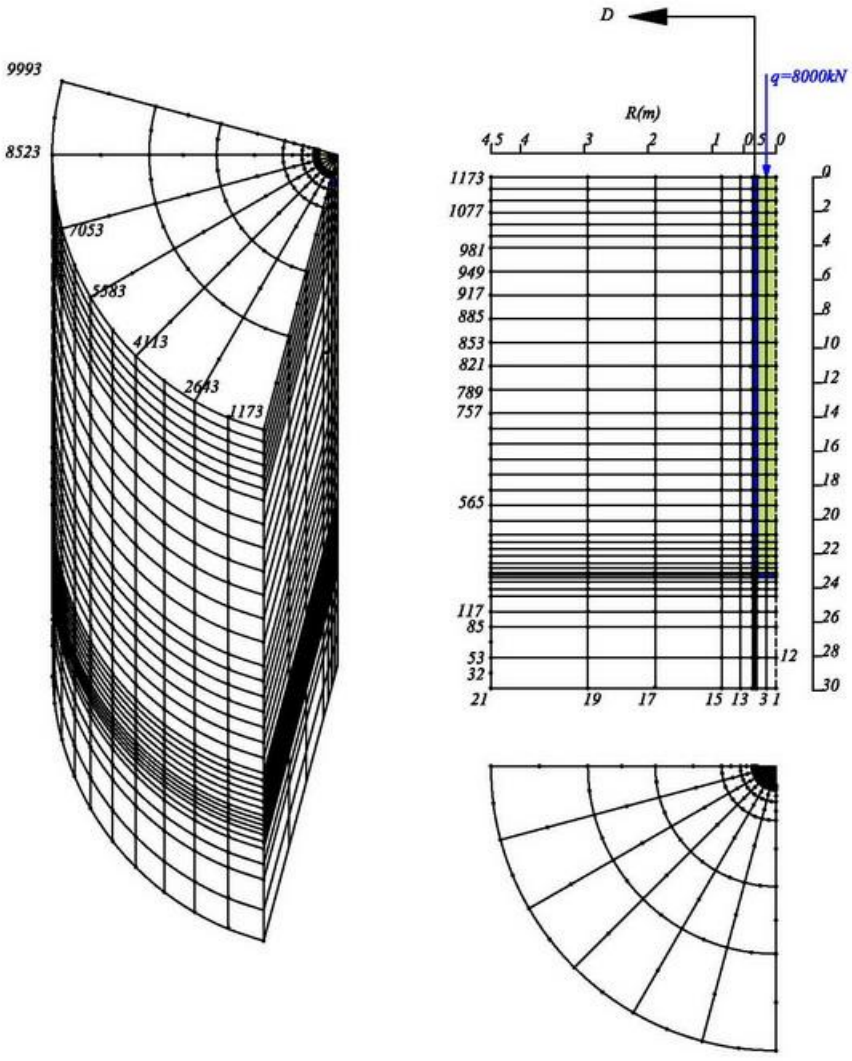

Figure (16) Finite element mesh for the single pile in clay after Seed and Reese, 1955.

i. For displacements at the tip of the pile, the maximum difference obtained at the end of loading is about 15%.
ii. For pore water pressure at a plane adjacent to and slightly away from the pile, the shapes of the dissipation curves of the pore water pressure isochrones were found similar to those obtained by Desai (1978).
2. A single pile driven in a clayey soil was analyzed by Ottaviani and Marchetti (1977). When applying the developed algorithm onto the problem, the following conclusions are reached:-
i. For displacements at the tip of the pile, the maximum difference obtained at the end of loading is about 8%.
ii. For pore water pressure at a plane adjacent to and slightly away from the pile, the trend of the dissipation of the pore water pressure is found comprehensible.

Soil Properties	
Property	**Value**
Undrained strength, $\mathbf{c_u}$	490 lb/ft^2 (23.5 kN/m^2)
Modulus of elasticity of the soil, $\mathbf{E_{soil}}$	44100 lb/ft^2 (2110 kN/m^2)
Poisson's ratio of the soil, $\mathbf{\nu_{soil}}$	0.35
The adhesion factor, $\boldsymbol{\alpha}$	1.0
Normal consolidation line slope, $\boldsymbol{\lambda}$	0.2
Shear modulus, **G**	15200 lb/ft^2 (725 kN/m^2)
Unit weight of the soil, γ_{soil}	110 lb/ft^3 (17.0 kN/m^3)
Permeability coefficient, $\mathbf{k_h=k_v}$	0.638×10^{-4} ft/day (0.2×10^{-4} m/day)
Pile Properties	
Property	**Value**
Modulus of elasticity of the pile, $\mathbf{E_{pile}}$	4.32×10^8 lb/ft^2 (2.1×10^7 kN/m^2)
Poisson's ratio of the pile, $\mathbf{\nu_{pile}}$	0.25
Unit weight of the pile, γ_{pile}	150 lb/ft^3 (23.5 kN/m^3)
Interface Element Properties	
Property	**Value**
Modulus of elasticity of the interface, $\mathbf{E_{interface}}$	44100 lb/ft^2 (2110 kN/m^2)
Poisson's ratio of the interface, $\nu_{interface}$	0.45
Unit weight of the interface, $\gamma_{interface}$	110 lb/ft^3 (17.0 kN/m^3)

Adhesion, $\mathbf{c_a}$	0.3 (kPa)
Wall friction angle, $\boldsymbol{\delta}$	30^o

Table (3) Material properties for case study number three (after Seed and Reese, 1955).

iii. The bearing resistance along the pile shaft and at the tip, and for different loading steps is found to be similar to those obtained by Ottaviani and Marchetti (1977).

3. Finally, a problem of a prototype pile in a clay soil tested by Seed and Reese (1955) is considered. When the same pile is analyzed by the algorithm developed in this research, namely ACED3, the following conclusions are reached:-

i. For displacements at the tip of the pile, the maximum difference at the end of loading is about 25%.

ii. For pore water pressure at a plane adjacent to and slightly away from the pile, the trend of the dissipation of the pore water pressure is found to be in line with respect to similar patterns of geometry, boundary and loading conditions.

iii. The bearing resistance along the pile shaft and at the tip, and for different loading steps, is found to be similar to those obtained by Seed and Reese (1955).

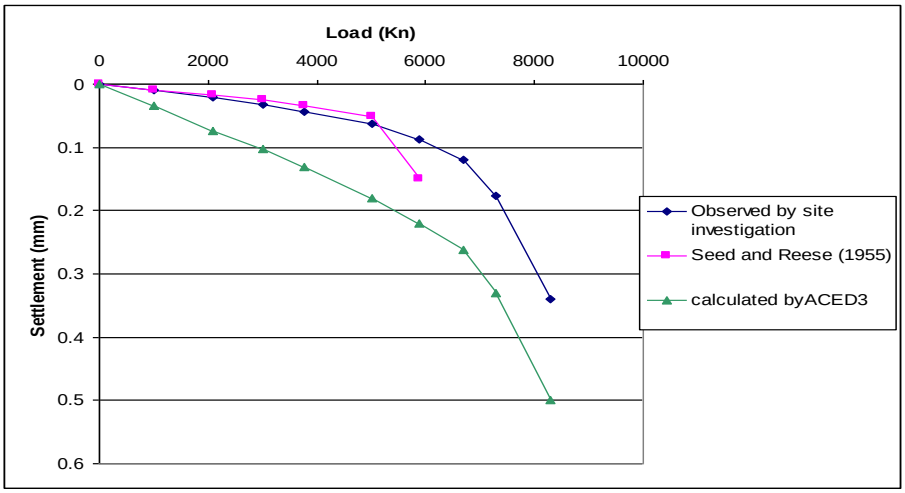

Figure (17) Load-settlement curve.

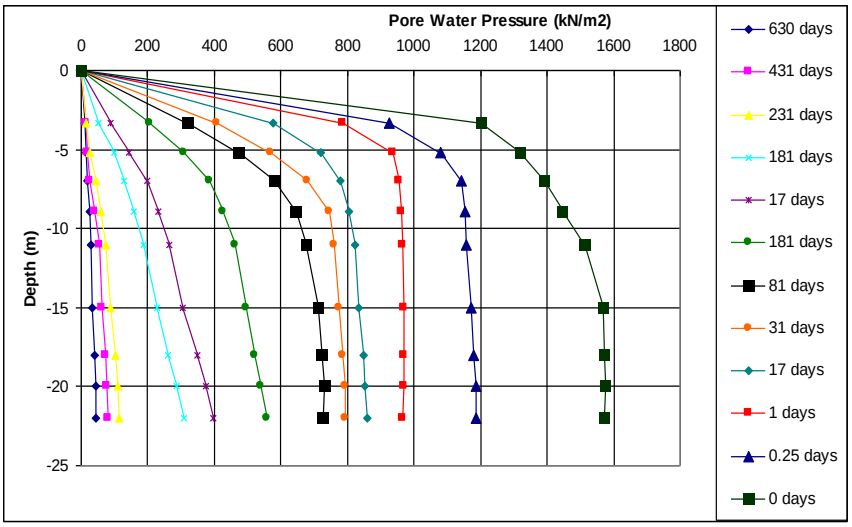

Figure (18) Pore water pressure dissipation.

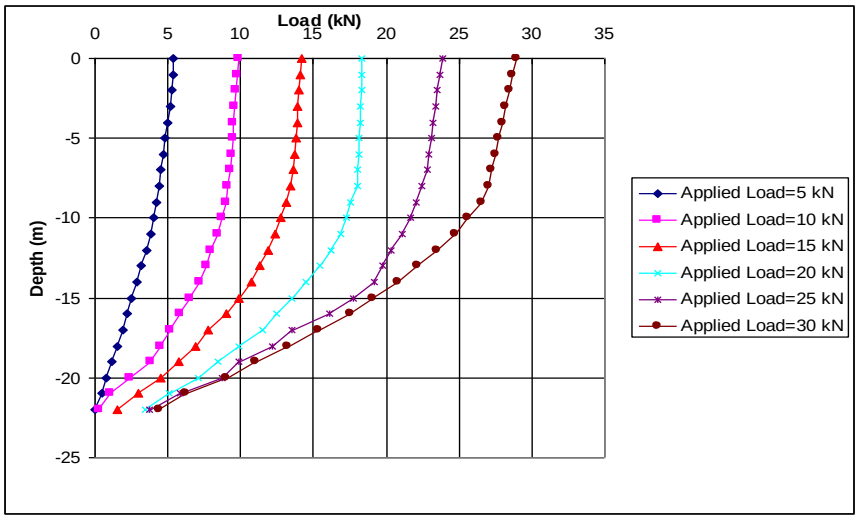

Figure (19) Load around the pile.

REFERENCES:

- Al-Anbaki, "**Three-Dimensional Analysis of Single Pile in Clay By The Finite Element Method**", A thesis submitted to the Department of Civil Engineering of the University of Baghdad for the degree of Master of Science, 2006.

- Al-Baghdadi, N. H., (2006), "**Soil-Pile Analysis by the Finite Element Method**", A thesis submitted to the Civil Eng. Dept. of the University of Kufa for the partial fulfillment of the degree of Masters of Science.

- Al-Damluji, O. F., (1981),"**Non-Linear Soil Behaviour by Finite Element Method**", M.Sc. Thesis, College of Engineering, University of Baghdad, Iraq.

- Al-Damluji, O. F. S., (1994), "**Dynamic Penetration Contact Problems with Particular Reference to Porous Media**", Ph.D. Thesis, College of Engineering, University of Baghdad.

- Al-Marsumi, M. R., (2003), "**The Effect of Time on Concrete Piles by Three-Dimensional Finite Element Analysis**", A thesis submitted to the Building and Construction Engineering Dept. of the University of Technology, Baghdad, for the partial fulfillment of the degree of Doctorate of Science.

- Atkinson J. H. and Bransby P.L., (1978); "**The Mechanics of Soils, An Introduction to Critical State Soil Mechanics**", McGraw-Hill Book Company, London, UK.

- Bathe, K. J., (1996), "**Finite Element Procedures**", Prentice-Hall International.

- Bhowmilk, S., and Long, J. H., (1990); "**Application of a Bounding Surface Plasticity Model in the Analysis of Axially Loaded Piles**", Proceedings of the Third International Conference on Numerical Methods in Engineering: Theory and Applications (NUMETA 90), 7-11 January, 1990, University College of Swansea, Swansea, Wales, U.K.

- Biot, M. A., (1955), "**Theory of Elasticity and Consolidation for a Porous Anisotropic Solid**", Journal of Applied Physics, Volume 26, pp. 182-185.

- Biot, M. A., (1956), "**Theory of Propagation of Elastic Waves in a Fluid Saturated Porous Solid**". Journal of the Acoustical Society of America, Volume 28, No. 2, March, pp.168-191.

- Cooke R. W., Price G. and Tarr K., (1979); "**Jacked Piles in London Clay: A Study of Load Transfer and Settlement under Working Conditions**", Geotechnique, Volume 29, No.2, P.P. 113-147.

- Desai, C. S., (1978). "**Effects of Driven and Subsequent Consolidation on Behaviour of Driven Piles**", International Journal for Numerical and Analytical Methods in Geomechanics, Vol. 2, pp.283-301.

- Desai, C. S., and Siriwardane, H. J. (1984), "Constitutive Laws for Engineering Materials with Emphasis on Geologic Materials", Prentice-Hall, Inc., Englewood Cliffs, New Jersey.

- Grande L. and Nordal S., (1979); "**Pile-Soil Interaction Analysis on Effective Stress Basis**", Recent Developments in the Design and Construction of Piles, ICE, London.

- Kirby R.C. and Esrig M.I., (1979); "**Further Development of a General Effective Stress Method for Prediction of Axial Capacity for Driven Piles in Clay**", Recent Developments in the Design and Construction of Piles, ICE, London.

- Kuhlemeyer, R., (1979), "**Bending Element for Circular Beams and Piles**", ASCE Journal of the Geotechnical Engineering Div, Volume: 105 Number: GT2, pp 325-330.

- Lewis, R. W. and Schrefler, B. A., (1987), "**The Finite Element Method in the Deformation and Consolidation of Porous Media**", John Wiley and Sons Ltd., London.

- Maharaj D. K., Gayatri J. and Jayanthi D., (2004); "**Uplift Capacity of Pile by the Finite Element Method**", Electronic Journal of Geotechnical Engineering, Vol. 8, P.P.414-420.

- Ottaviani, M., and Marchetti, S., (1979), "**Observed and Predicted Test Pile Behaviour**", International Journal for Numerical Methods in Geomechanics, Vol. 3, pp. 131-143.

- Owen, D. R. J., and Hinton, E., (1980), "**Finite Elements in Plasticity-Theory and Practice**", Pineridge Press Ltd., Swansea.

- Pal S.C and Parikh S. K., (1980); "**Linear Axi-Symmetric Finite Element Analysis of Concrete Piles in Nonhomogenous Clay Soil**", Journal of Indian Geotehnique, No.3, vol.10, P.P. 185-202.

- Phoon, K. K., Quek, S. T., Chow, Y. K., and Lee, S. L., (1990) "**Reliability Analysis of Pile Settlement**", Journal of Geotechnical Engineering, ASCE, Vol. 116, No. 11, November 1990, pp. 1717-1735.

- Raheem, A. M., (2005), "**Pile-Soil Interaction Analysis on Effective Stress Basis**", a thesis submitted to Civil Eng. Dept. of the University of Baghdad for the partial fulfillment of the degree of Masters of Science.

- Randolph M. F. and Wroth C. P., (1978); "**Analysis of Deformation of Vertically Loaded Piles**", Geotechnique, Vol. 104, No. 12, P.P. 1465-1488.

- Randolph M.F., Carter J.P. and Wroth, (1979); "**Driven Piles in Clay-The Effects of Installation and Subsequent Consolidation**", Geotechnique, Vol. 29, No.4, P.P. 361-393.

- Reddy, J. N., (1984), "**An Introduction to the Finite Element Method**", McGraw-Hill International Editions.

- Saada, A. S., (1974), "**Elasticity, Theory and Application**", Pergamon Press Inc.

- Seed, H. B., and Reese, L. C., (1955), "**The Action of Soft Clay along Friction Piles**", Transactions of the ASCE, Vol. 23, No. 122, P.P. 731-754.

- Smith, I. M. and Griffiths, D. V., (1988), "**Programming the Finite Element Method**", 2nd Edition, John Wiley and Sons. Inc.

- Yasser, A. K. and Hassiotis, S., (2001); "**Analysis of Pile Soil Interaction**", Geotechnique, Vol. 22, No. 4, P.P. 103-115.

LIST OF SYMBOLS:

α : time integration constant.

α: adhesion factor.
$\gamma_{interface}$: Unit weight of the interface.
$\gamma_{pile:}$ Unit weight of the pile.
$\gamma_{soil:}$ Unit weight of the soil.
Δt_k: length of the k-th time step.
δ : Wall friction angle.
δε: small changes in strain.
δσ': small changes in effective stress.
δλ: a positive scalar factor of proportionality dependent on the state of stress and loading history.
$\{\delta_i\}$: vector of nodal displacements of node (i).
λ: normal consolidation line slope.
ξ, , η and ζ are the finite element local coordinates as defined by Figure (1).
ν: Poisson's ratio.
$\nu_{interface}$: Poisson's ratio of the interface.
$\nu_{pile:}$ Poisson's ratio of the pile,
$\nu_{soil:}$ Poisson's ratio of the soil.
σ_n, σ, σ_{nn}: normal stress.
σ'_{mo}: isotropic effective stress.
σ'_x , σ'_y, σ'_z: effective stresses in the x, y and z directions, respectively.
σ_x, σ_y, σ_z: total stress increments in x, y ,z directions, respectively.
σ_1, σ_2, σ_3: principal stresses acting on right angles to each other.
Ω: total domain of the continuum.
[B]: strain-nodal displacement matrix (transformation matrix).
B: bulk modulus
C: creep function.
c_a : Adhesion.
c_u : Undrained strength.
[D]: stress-strain (constitutive) matrix.
dΩ: domain of the integration.
dε: total strain of the skeleton.
$E_{interface:}$ Modulus of elasticity of the interface.
$E_{pile:}$ Modulus of elasticity of the pile.
$E_{soil:}$ Modulus of elasticity of the soil.
$d\varepsilon_c$: creep strain.
$d\varepsilon_p$: overall volumetric strains caused by uniform compression of the particles by the pressure of the pore fluid.
$d\hat{f}$: change in external force due to boundary and body force loadings.
df: load vector equivalent to the body force, surface traction and autogenous strain, respectively.
E: modulus of elasticity of soil skeleton.
f: yield criterion.
$\bar{f}$: load vector equivalent to fluid flow of source elements, creep function and gravity load, respectively.
{F}: vector of nodal forces,

G: shear modulus.
H: spatial flow (or seepage) matrix applied in three dimension form.
[J], $[J]^e$: Jacobian matrix in Cartesian coordinates.
K: Bulk modulus.
K_0: earth pressure coefficient at rest.
[K] : stiffness matrix.
$\mathbf{k_h}$,$\mathbf{k_v}$: horizontal and vertical permeability coefficients, respectively.
L: coupling matrix representing the influence of pore pressure in force equilibrium.
m: number of nodes per element.
$\mathbf{M_{cs}}$: the slope of the critical state line.
$\{N_i\}$ = interpolation function of nodal point (i).
$\overline{\mathbf{p}}$: pore pressures.
p: pore water pressure.
p′: mean effective stress.
$\mathbf{p_c'}\left(\boldsymbol{\varepsilon_v^p}\right)$ is the preconsolidation pressure to which the soil has previously been subjected to during its past history. The superscript p for volumetric strain is for plastic.
q: deviatoric stress.
S: compressibility matrix.
t: time of consolidation.
u: displacement vector.
ū: displacements.
$\{X_i\}$: vector of coordinates of nodal point (i).
the superscript ($^{\mathbf{T}}$) represents the transpose of the matrix.